Acta Crystallographica Section B
Structural Science
ISSN 0108-7681

$LiNaSiB_3O_7(OH)$ – novel structure of the new borosilicate mineral jadarite determined from laboratory powder diffraction data

Pamela S. Whitfield,[a]* Yvon Le Page,[a] Joel D. Grice,[b] Chris J. Stanley,[c] Gary C. Jones,[c] Michael S. Rumsey,[c] Chris Blake,[d] Andrew C. Roberts,[e] John A. R. Stirling[e] and Gordon J. C. Carpenter[f]

[a]ICPET, National Research Council, 1200 Montreal Road, Ottawa, Ontario, Canada K1A 0R6, [b]Canadian Museum of Nature, PO Box 3443, Stn D, Ottawa, Ontario, Canada K1P 6P4, [c]Department of Mineralogy, Natural History Museum, London SW7 5BD, England, [d]Rio Tinto, Unit 34, Hither Green Industrial Estate, Clevendon, Somerset BS21 6XU, England, [e]Geological Survey of Canada, 601 Booth Street, Ottawa, Ontario, Canada K1A 0E8, and [f]Materials Technologies Laboratories, Natural Resources Canada, 568 Booth Street, Ottawa, Ontario, Canada K1A 0G1

Correspondence e-mail: pamela.whitfield@nrc.gc.ca

Received 18 January 2007
Accepted 2 March 2007

The structure of a new mineral jadarite, $LiNaSiB_3O_7(OH)$ (IMA mineral 2006–36), has been determined by simulated annealing and Rietveld refinement of laboratory X-ray powder diffraction data. The structure contains a layer of corner-sharing, tetrahedrally coordinated Li, Si and B forming an unbranched vierer single layer, which is decorated with triangular BO_3 groups. The Na ion is situated between the tetrahedral layers in a distorted octahedral site. As the very high boron content in this mineral makes obtaining neutron diffraction data very problematic, *ab initio* optimization using *VASP* was used to validate the structure and to better localize the H atom. The H atom is located on the apex of the triangular BO_3 group and is involved in a weak intralayer hydrogen bond. The final Rietveld refinement agrees with the *ab initio* optimization with regard to a hydrogen bond between the H atom and one of the tetrahedral corner O atoms. The refined structure seems to be of a remarkably high quality given the complexity of the structure, the high proportion of very light elements and the fact that it was determined from relatively low-resolution laboratory data over a limited 2θ range (10–90° 2θ).

1. Introduction

$LiNaSiB_3O_7(OH)$ is a new mineral phase named jadarite (IMA number 2006–36) that was discovered in a drill-core from a borehole in the Jadar Basin in Serbia. A full description of the mineral and its characteristics will appear in Stanley *et al.* (2007). It occurs as agglomerates of small plate-like crystals that rarely exceed 5 μm in size. The small size of the individual crystals severely limits the applicability of single-crystal diffraction, so an attempt was made to solve the structure using powder diffraction data.

Most mineral crystal structures are determined from single-crystal techniques, but some mineral structures are found using powder data, for example tinticite (Rius *et al.*, 2000) and kanemite (Vortmann *et al.*, 1999). Most structure determinations from powder data use high-resolution synchrotron data (Wallwork *et al.*, 2003), but laboratory data has been used successfully, usually for simpler, high-symmetry structures (Tettenhorst & Corbato, 1984; Plaisier *et al.*, 1995), but triclinic structures have also been solved successfully (Rius *et al.*, 2000).

H atoms can be very difficult to locate within structures using X-ray powder diffraction alone. Neutron diffraction of a deuterium-substituted sample would be the conventional method for accurately locating H atoms experimentally. However, in this case the high boron content makes obtaining neutron diffraction data extremely difficult because of the very high neutron absorption cross section of ^{10}B. An alter-

Table 1
Experimental details.

Crystal data	
Chemical formula	$B_3HO_8Si{\cdot}NaLi$
M_r	219.46
Cell setting, space group	Monoclinic, $P2_1/c$
Temperature (K)	298
a, b, c (Å)	6.7620 (1), 13.8016 (3), 7.6878 (2)
β (°)	124.089 (1)
V (Å^3)	594.18 (2)
Z	4
D_x (Mg m^{-3})	2453
Radiation type	Cu $K\alpha$
μ (mm^{-1})	4.51
Specimen form, colour	Powder, white
Specimen size (mm)	16 × 0.5 × 0.5
Specimen preparation cooling rate (K min^{-1})	N/A
Specimen preparation pressure (kPa)	N/A
Specimen preparation temperature (K)	N/A
Data collection	
Diffractometer	Bruker D8 Advance
Data collection method	Specimen mounting: quartz capillary; mode: transmission; scan method: continuous
Absorption correction	For a cylinder mounted on the φ axis
T_{min}	N/A
T_{max}	N/A
2θ (°)	$2\theta_{min}$ = 15, $2\theta_{max}$ = 90, increment = 0.01641
Refinement	
Refinement on	F^2
R factors and goodness-of-fit	R_p = 0.028, R_{wp} = 0.042, R_{exp} = 0.016, R_B = 0.013, S = 1.27
Wavelength of incident radiation (Å)	1.5418
Excluded region(s)	N/A
Profile function	Fundamental parameters convolution-based profiles in *TOPAS*
No. of parameters	87
H-atom treatment	Mixture of independent and constrained refinement
Weighting scheme	Unit
$(\Delta/\sigma)_{max}$	0.001

Computer programs used: *TOPAS*4 beta (Bruker AXS, 2006), *DIAMOND*3.1d (Bergerhoff *et al.*, 1996).

native approach to locating the H atoms within structures is the use of quantum chemical calculations (Kaduk, 2002). In addition, the ability to reproduce, or not reproduce, the experimental cell data through *ab initio* optimization of a tentative structure model constitutes a powerful argument for or against the validity of the corresponding model, even in the absence of a competing model (Le Page *et al.*, 2002).

2. Experimental

The density of the mineral was measured as 2.45 g cm^{-3} using a Berman balance (Stanley *et al.*, 2007). Elemental analysis by wet chemical methods and quantitative electron microprobe yielded an empirical formula of $Li_{1.08}Na_{1.07}Si_{0.97}B_3O_{6.99}(OH)_{1.06}$ on the basis of three B atoms per formula unit. This composition has been simplified to $LiNaSiB_3O_7(OH)$. IR absorption spectroscopy results suggested the presence of triangular borate groups (Stanley *et al.*, 2007), as well as the expected tetrahedral BO_4 groups.

2.1. Data collection

The original $LiNaSiB_3O_7(OH)$ sample was ground into a fine powder before loading into a 0.5 mm diameter quartz capillary. Data were collected on a Bruker D8 Advance diffractometer using a primary Goebel mirror with a 0.6 mm exit slit and a Vantec PSD detector. The detector was equipped with radial Soller slits, and was used with a 3° detector window. Data were collected between 10 and 90° 2θ using the equivalent of a 0.0164° step size and a 10 s count time. Cu $K\alpha$ radiation was used, but no Ni filter was necessary since the primary mirror removes the $K\beta$ component. The instrument profile and calibration was measured using a 0.5 mm diameter quartz capillary with SRM640b silicon. Full experimental details are given in Table 1.

2.2. Data processing and structure determination

All data processing was carried out using a beta version of *TOPAS*4.0 (dated 25/6/2006; Bruker AXS, 2006). The data from the SRM640b silicon were used to model the instrument function for further peak fitting. Convolution-based profile fitting was used for all the work. Peak positions were determined using single peak fitting. The individual peaks were all constrained with the same size broadening in order to highlight possible peak overlaps. There were 42 reflections, up to 60° 2θ, which were used as input into the singular-value decomposition-indexing algorithm (Coelho, 2003) in *TOPAS*. The maximum ratio of calculated to observed reflections (N_c/N_o) was varied between 3 and 12.

The structure solution was undertaken with simulated annealing in *TOPAS*. The SiO_4 unit was described as a tetrahedral z matrix with allowable Si—O bond lengths between 1.60 and 1.65 Å. It was not possible to locate the H atom individually, so it was attached to one of the O atoms with a 0.96 Å bond length, and refined as an (OH) unit. The other atoms were refined individually. Soft bond-length constraints between cations and O atoms were used, together with a number of anti-bump constraints that were also used between the different cations. The bond-length constraints used approximately corresponded to those bond lengths expected from bond-valence considerations. In order to decrease the calculation time, the *TOPAS* option of using the peak intensities, known in the software as 'decomposition', was used instead of synthesizing peak profiles.[1]

The Rietveld refinements were carried out using a 5 times greater weighting for the reflections above 39° 2θ, with a 2 degree overlap between 1× and 5× weighted portions. This pseudo-variable count time approach was used to extract more structural details than a conventional refinement might support. Other than structural and microstructural variables

[1] Supplementary data for this paper are available from the IUCr electronic archives (Reference: LM5008). Services for accessing these data are described at the back of the journal.

Table 2
Bond-valence analysis for the $LiNaSiB_3O_7(OH)$ structure.

Atom	Average bond length (Å)	Bond valence
Li	1.929 (23)	1.1
Na	2.484 (14)	1.0
Si	1.586 (10)	4.6
B1	1.513 (26)	2.7
B2	1.518 (21)	2.7
B3	1.379 (12)	2.9

(unit cell, atomic positions, isotropic displacement parameters, Lorentzian crystallite size, Gaussian microstrain), corrections for zero-point error and cylindrical absorption were also refined. Additionally, anisotropic displacement parameters were refined for the Na ion and one of the B atoms in the structure. The displacement parameter of the H atom was fixed to 1.3 times the parameter of the connected O8 atom. To keep the hydrogen position within a reasonable range, the O8—H bond length was soft-constrained to a distance of 0.96 Å. All other bond-length constraints were removed for the final refinement.

The stability of the final structure refinement and parameter correlation was examined by analysing the least-squares normal matrix with the program *SVDdiagnostic* (Mercier *et al.*, 2006).

2.3. *Ab-initio* optimization

The refined structure was validated and the H atom located in the structure using *ab initio* optimization. In this perspective, we have undertaken the *ab initio* optimization of the X-ray cell and structure results from the initial Rietveld refinement. Input data files for *VASP* (Kresse, 1993; Kresse & Hafner, 1993, 1994) were generated by *Materials Toolkit* (Le Page & Rodgers, 2005) from CIF files output by *TOPAS*4.0. From valence summation (Brown & Altermatt, 1985), it was clear that the H atom had to be attached to the O8 atom. Input files were prepared for several stereochemically plausible positions for the H atom. *Ab initio* optimizations with VASP used the following execution parameters: GGA PAW potentials (Kresse & Joubert, 1999); electronic convergence at 1×10^{-7} eV; convergence for forces of 1×10^{-4} eV Å^{-1}; Davidson-blocked iterative optimization of the wavefunctions in combination with reciprocal-space projectors (Davidson, 1983); reciprocal space integration with a Monkhorst–Pack scheme (Monkhorst & Pack, 1976); a Methfessel–Paxton smearing scheme of the order 1 and width 0.2 eV for energy corrections (Methfessel & Paxton, 1989). Spin-polarization corrections were not used. The *k*-mesh grid used was $3 \times 2 \times 3$. A total of 50 single-point energy-minimization iterations was completed for each simulation to ensure proper convergence of atom relaxation, calculated energy and stress. The calculations required about 5 d each on single 3 GHz Athlon-64 PCs running serial *VASP*4.6.3 under Microsoft® Windows® XP Professional, using the execution scheme described above.

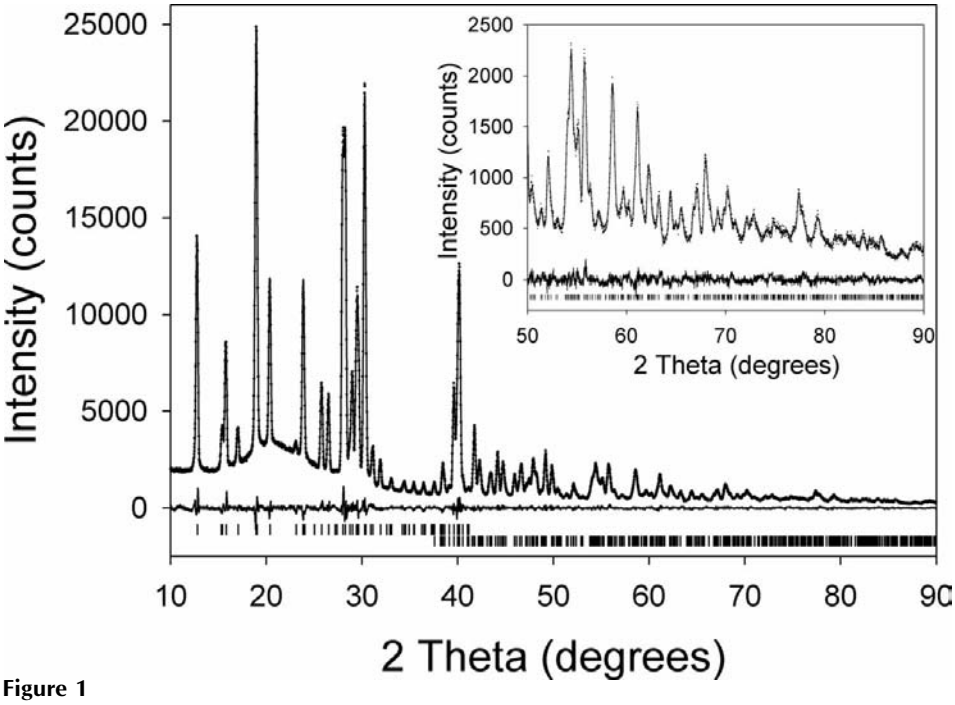

Figure 1
Difference plot for the final refinement of $LiNaSiB_3O_7(OH)$. The inset shows a blow-up of the higher-angle region.

3. Results and discussion

The best indexing solution (GOF = 13.05) was found with a maximum N_c/N_o ratio of 7 in the space group $P2_1/c$. A Pawley fit of this cell to the experimental data refined to a = 6.7651 (2), b = 13.8063 (5), c = 7.6912 (2) Å, β = 124.099 (1)° with a fit of R_{wp} = 0.036. This unit cell and space group corresponds to the Parthé standard setting of a monoclinic cell (Parthé & Gelato, 1984, 1985).

The simulated annealing was stopped when a possible solution with an R_{wp} value of 0.175 was found. Visual inspection of the structure yielded a number of tetrahedra and a triangular coordinated B atom. Given the suggested presence of three-coordinate B from the IR absorption data, a refinement of this structure was attempted. This refinement ultimately yielded a background-subtracted R'_{wp} value of 0.077 using isotropic displacement parameters. From laboratory powder diffraction data, confidence in the location and bonding of the H atom from this refine-

ment was quite low. Consequently, these interim refined positions were optimized using *VASP*.

One of the structures with different H-atom positions gave, after *ab initio* optimization, a total energy that was 0.4 eV lower than the next best structure, which is very significant. The corresponding optimized cell deviated least from the experimental one and the structure also displayed a straight hydrogen bond to O3. The resulting optimized atomic coordinates and cell parameters are summarized in Table 1 of the supplementary data. The H atom was placed in the corresponding position for the experimental cell for the final refinement.

The final refinement with 87 variables yielded an overall background-subtracted R_{wp} value of 0.0699 (conventional R_{wp} = 0.0418) and an R_B of 0.0127. The fit and difference plot is shown in Fig. 1. Analysis of the least-squares normal matrix yielded a $\log_{10}$(condition number) of 10 and 2 for the unprocessed and preconditioned matrices (Mercier *et al.*, 2006), respectively. Together with a Durban–Watson statistic of 1.765, this indicated that there were no serious parameter correlations and gave confidence in the stability and reliability of the refinement. The refined phase density was 2.45321 (9) g cm^{-3}, which is in excellent agreement with the measured density. The structural parameters extracted from the refinement are shown in Table 2 of the supplementary data. Given the very high proportion of light elements in this naturally occurring mineral phase and the complexity of the structure, the stability of the refinement and the relatively small e.s.d.s with such a large number of variables is surprising. Despite all the other satisfactory residuals, the overall goodness-of-fit reported by *TOPAS* was 2.7, which is quite poor. This high GOF can occur when the counting statistics of the data are good enough that the misfit between observed and calculated patterns becomes very large when compared with uncertainties in the intensities (Toby, 2006). If this is the case, a more realistic goodness-of-fit may be calculated using the R_{wp} value of a structure-less Pawley fit to the same data (Toby, 2006), as opposed to the conventional R_{exp}. In this case the R_{wp} of the Pawley fit was 0.033, giving a goodness-of-fit using $R_{exp} = R_{wp(Pawley)}$ of 1.27.

Fig. 2 shows a polyhedral representation of the $LiNaSiB_3O_7(OH)$ structure viewed along the [001] direction. The structure consists of a two-dimensional layer made up of corner-sharing borosilicate tetrahedra parallel to (010). The hole within this layer is partially filled by a LiO_4 tetrahedron. The inter-tetrahedral layer contains six-coordinate Na and triangular-coordinated B, which share corners of the two BO_4 and the LiO_4 tetrahedra. Following the silicate classification terminology (Liebau, 1985), the borosilicate tetrahedral network is an unbranched vierer single layer with a B_2SiO_7 layer composition (Fig. 3). The layer may be described as edge-sharing six- and fourfold rings with a net topology of $(6^2{\cdot}4^2)(6^2{\cdot}4)_2$ (Fig. 4). This net topology is only for the BO_4 and SiO_4 polyhedra. Within the borosilicate minerals (62 species), none were found that resemble that of $LiNaSiB_3O_7(OH)$. Looking to non-borosilicate phases, aminoffite, $Ca_3Be_2Si_3O_{10}(OH)_2$, has a two-dimensional tetrahedral layer of six- and fourfold rings, but the topology, $(6^4)(6^2{\cdot}4)_2$ (Grice & Hawthorne 2002), differs from that of the structure described here. The only phase with a net topology matching that of $LiNaSiB_3O_7(OH)$ is $Ba_2CuSi_2O_7$ (Malinovskii, 1984) with Cu having a tetrahedral coordination. The H atom is bonded to the O8 atom at the apex of the BO_3 group, which is shared with the LiO_4 tetrahedra. The refined H1 position did not move markedly from that derived from the *ab initio* optimization. The O8—H1 bond is approximately pointed along the [201] direction parallel to the plane of the BO_3 plane

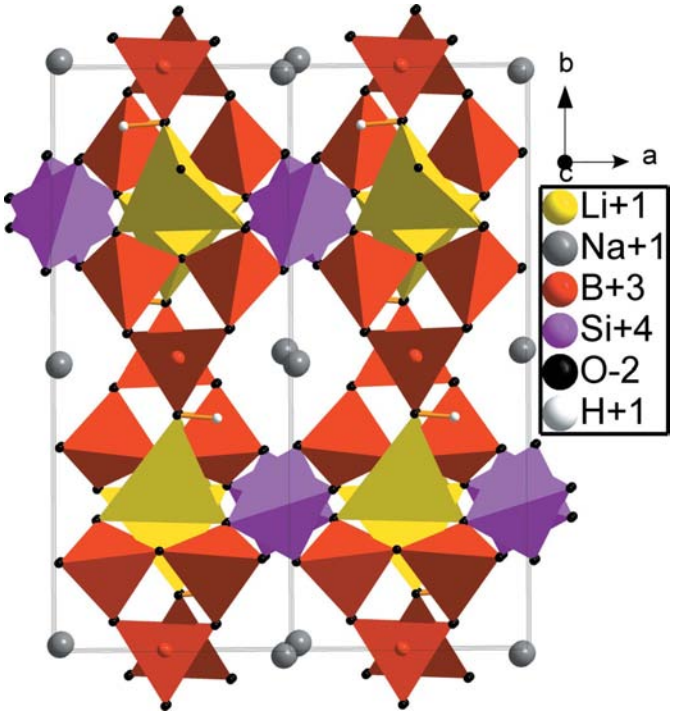

Figure 2
Polyhedral representation along the *c* axis of the structure of $LiNaSiB_3O_7(OH)$.

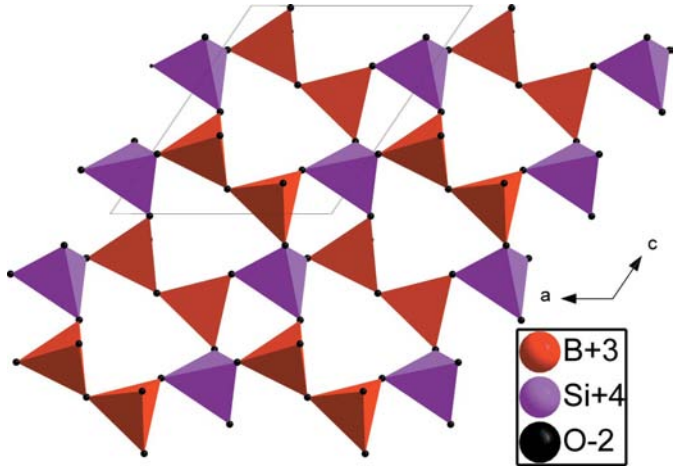

Figure 3
Polyhedral representation of the B_2SiO_7 single layers

and still forms a hydrogen bond to the O3 atom as shown in Fig. 5.

The significant elongation of the anisotropic displacement parameters of the B3 atom are illustrated in Fig. 6. These were refined owing to the possible movement of the B atom out of the triangular plane of the BO_3 unit. The successful refinement of anisotropic displacement parameters with acceptable estimated standard deviations (e.s.d.s) from laboratory X-ray powder data for such a light element is somewhat unusual. The size and shape of the ellipsoid is not unexpected, but the direction has a significant in-plane component, which has no apparent structural cause. It may be due to the unavoidable simplification in this study of a naturally occurring phase that has inherent inhomogeneities. The microstructural parameters in the refinement produce a non-zero microstrain, even using the strained SRM640b as the instrument standard, which may be an indication of such imperfections. The displacement parameters for the Na ion do not have a pronounced elongation, although there is some movement towards averaging the positional zigzag along the *c* axis which is apparent in Fig. 2.

Results of bond-valence calculations for the cations are shown in Table 2. The calculated bond-valence parameters are reasonable given the inherently larger errors in the bond lengths from laboratory powder diffraction of such a material. Six-coordinate Na in a mineral structure is somewhat unusual, so attempts were made to see whether the Na ion could be forced to have a higher coordination number. In each case, this resulted in unacceptable distortions in the corner-sharing tetrahedral network. The possibility of partial occupancy of the heavier cations was also examined. Refinements of the Na and Si occupancies did not yield values below 1.0.

Mineralogists may wish to describe this structure using the reduced non-Parthé cell in the alternative space group $P2_1/n$ [a = 6.8300 (1), b = 13.8051 (2), c = 6.7620 (1) Å, β = 111.072 (1)°]. The $P2_1/n$ structure may be derived from $P2_1/c$, using the matrix transformation $a + c$, b, $-a$.

4. Conclusions

The structure of a new mineral jadarite, with the ideal formula $LiNaSiB_3O_7(OH)$ has been solved from laboratory powder diffraction data. The structure was validated and the H atom located using *ab initio* optimization with *VASP*. The structure has a two-dimensional corner-sharing tetrahedral network with Li, Si and two B atoms forming an unbranched vierer single layer. The layers are bound together by a three-coordinate triangular B atom and a six-coordinate Na ion. Notable features of the structure (Na channels, 'LiO_4', SiO_4, BO_3 chains, *etc*) occur roughly parallel to the *c* axis, whilst the borosilicate layers lie in the (001) plane. The H atom is bound to one of the O atoms in the triangular BO_3 unit, and forms a hydrogen bond to one of the O atoms in the tetrahedral network. The structure appears to be unique and has no known direct structural analogues.

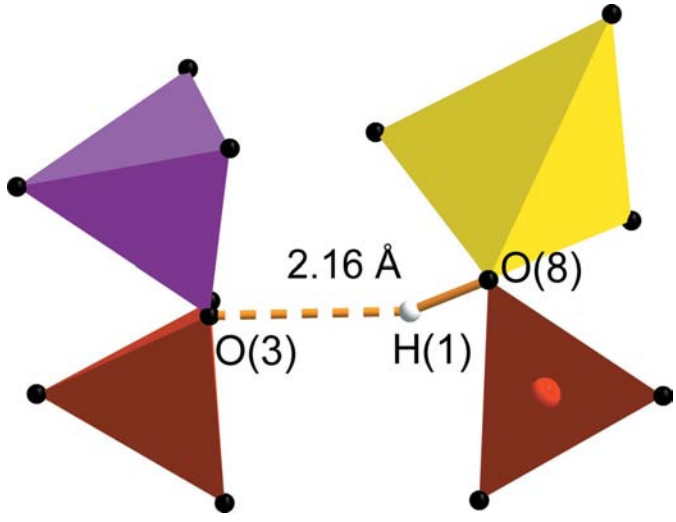

Figure 5
Diagram showing the hydrogen bond to O3.

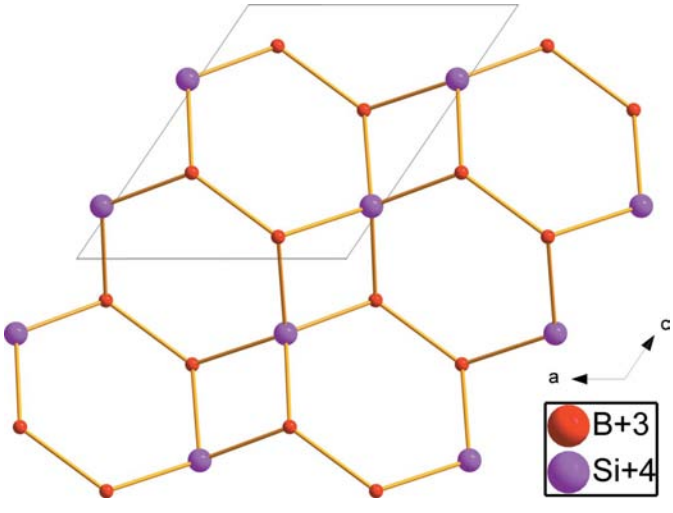

Figure 4
The $(6^2{\cdot}4^2)(6^2{\cdot}4)_2$ net topology of the B_2SiO_7 layers

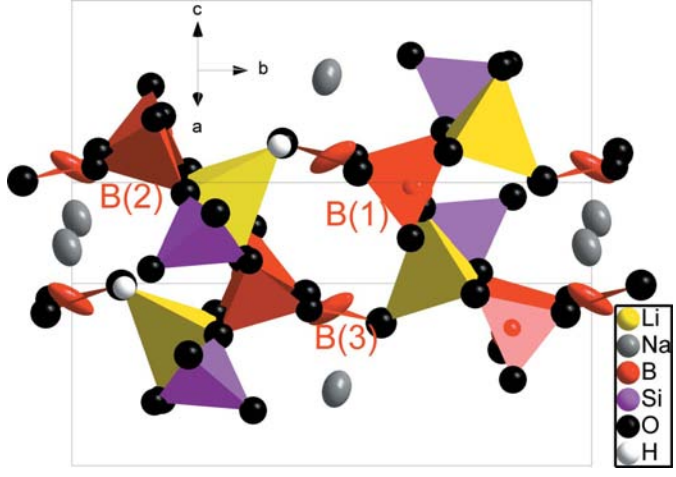

Figure 6
View along the 301 plane showing the displacement of the B3 and Na atoms. The ellipsoids are shown for 50% probability.

The following people from the Rio Tinto Industrial Minerals Exploration staff are acknowledged for their contribution in discovering this new mineral: Vladimir Stojanović, Vladisav Erić, Rodrigo Calles-Montijo, Robert Kellie, William Pennell & Nenad Grubin. PSW would also like to thank Dr Arnt Kern and Dr Alan Coelho with Bruker-AXS GmbH for the continued opportunity to explore the latest *TOPAS* beta versions.

References

Bergerhoff, G., Berndt, M. & Brandenburg, K. (1996). *J. Res. Natl Inst. Stand. Technol.* **101**, 221–225.
Brown, I. D. & Altermatt, D. (1985). *Acta Cryst.* B**41**, 244–247.
Bruker AXS (2006). *TOPAS*. Bruker AXS, Karlsruhe, Germany.
Coelho, A. A. (2003). *J. Appl. Cryst.* **36**, 86–95.
Davidson, E. R. (1983). *Methods in Computational Molecular Physics*, edited by G. H. F. Diercksen & S. Wilson, Vol. 113, pp. 95, NATO Advanced Study Institute, Series C. New York: Plenum Press.
Grice, J. D. & Hawthorne, F. C. (2002). *Can. Mineral.* **40**, 971–980.
Kaduk, J. A. (2002). *Acta Cryst.* B**58**, 815–822.
Kresse, G. (1993). PhD thesis. Technische Universita Wien, Austria.
Kresse, G. & Hafner, J. (1993). *Phys. Rev. B*, **48**, 13115–13118.
Kresse, G. & Hafner, J. (1994). *Phys. Rev. B*, **49**, 14251–14269.
Kresse, G. & Joubert, J. (1999). *Phys. Rev. B*, **59**, 1758–1775.
Le Page, Y. & Rodgers, J. R. (2005). *J. Appl. Cryst.* **38**, 697–705.
Le Page, Y., Saxe, P. S. & Rodgers, J. R. (2002). *Acta Cryst.* B**58**, 349–357.
Liebau, F. (1985). *Structural Chemistry of Silicates: Structure, Bonding and Classification.* Berlin: Springer-Verlag.
Malinovskii, Yu. A. (1984). *Dokl. Acad. Nauk SSSR*, **278**, 616–619.
Mercier, P. H. J., Le Page, Y., Whitfield, P. S. & Mitchell, L. D. (2006). *J. Appl. Cryst.* **39**, 458–465.
Methfessel, M. & Paxton, A. T. (1989). *Phys. Rev. B*, **40**, 3616–3621.
Monkhorst, H. J. & Pack, J. D. (1976). *Phys. Rev. B*, **13**, 5188–5192.
Parthé, E. & Gelato, L. M. (1984). *Acta Cryst.* A**40**, 169–183.
Parthé, E. & Gelato, L. M. (1985). *Acta Cryst.* A**41**, 142–151.
Plaisier, J. R., Jansen, J., de Graaf, R. A. G. & Ijdo, D. J. W. (1995). *J. Solid State Chem.* **115**, 464–468.
Rius, J., Louer, D., Louer, M., Gali, S. & Melgarejo, J. C. (2000). *Eur. J. Mineral.* **12**, 581–588.
Stanley, C. J., Jones, C. G., Rumsey, M., Blake, C., Roberts, A. C., Stirling, J. A. R., Carpenter, G. C. J., Whitfield, P. S., Grice, J. D. & Le Page, Y. (2007). *Eur. J. Mineral.* In the press.
Tettenhorst, R. T. & Corbato, C. E. (1984). *Am. Mineral.* **69**, 943–947.
Toby, B. H. (2006). *Powder Diffr.* **21** 67–70.
Vortmann, S., Rius, J., Marler, B. & Gies, H. (1999). *Eur. J. Mineral.* **11**, 125–134.
Wallwork, K. S., Pring, A., Taylor, M. R. & Hunter, B. A. (2003). *Am. Mineral.* **88**, 235–239.